Regional modeling of decadal rainfall variability over the Sahel

Deborah Herceg · Adam H. Sobel · Liqiang Sun

Abstract A regional climate model is used to investigate the mechanism of interdecadal rainfall variability, specifically the drought of the 1970s and 1980s, in the Sahel region of Africa. The model is the National Center for Environmental Prediction's (NCEPs) Regional Spectral Model (RSM97), with a horizontal resolution of approximately equivalent to a grid spacing of 50 km, nested within the ECHAM4.5 atmospheric general circulation model (AGCM), which in turn was forced by observed sea surface temperature (SST). Simulations for the July–September season of the individual years 1955 and 1986 produced wet conditions in 1955 and dry conditions in 1986 in the Sahel, as observed. Additional July–September simulations were run forced by SSTs averaged for each month over the periods 1950–1959 and the 1978–1987. These simulations yielded wet conditions in the 1950–1959 case and dry conditions in the 1978–1987 case, confirming the role of SST forcing in decadal variability in particular. To test the hypothesis that the SST influences Sahel rainfall via stabilization of the tropospheric sounding, simulations were performed in which the temperature field from the AGCM was artificially modified before it was used to force the regional model. We modified the original 1955 ECHAM4.5 temperature profiles by adding a horizontally uniform, vertically varying temperature increase, taken from the 1986–1955 tropical mean warming in either the AGCM or the NCEP/National Center for Atmospheric Research Reanalysis. When compared to the 1955 simulations without the added tropospheric warming, these simulations show a drying in the Sahel similar to that in the 1986–1955 difference and to the decadal difference between the 1980s and 1950s. This suggests that the tropospheric warming may have been, at least in part, the agent by which the SST increases led to the Sahel drought of the 1970s and 1980s.

1 Introduction

The Sahel region of West Africa is highly vulnerable to climate variability. In the latter half of the twentieth century, the Sahel experienced significant rainfall variability on both interannual and decadal time scales. The 1950s and 1960s were anomalously wet, and the 1970s and 1980s were anomalously dry, with serious consequences for the region's populations. One hypothesis for the decline in rainfall which occurred between the 1950s and 1980s invokes land use change, leading to albedo changes and "desertification" (Charney 1975). However, recent work points to the influence of changes in sea surface temperature (SST) over the tropical oceans (Lough 1986; Giannini et al. 2003; Folland et al. 1986; Palmer 1986; Thiaw et al.

D. Herceg (✉)
Institute of Marine and Coastal Sciences (IMCS),
Rutgers University, 71 Dudley Road,
New Brunswick, NJ 08901, USA
e-mail: herceg@marine.rutgers.edu

A. H. Sobel
Department of Applied Physics and Applied Mathematics,
Department of Earth and Environmental Sciences,
Columbia University, New York, NY, USA

A. H. Sobel · L. Sun
International Research Institute for Climate and Society
(IRI), Columbia University, Palisades, NY, USA

2005) and the Mediterranean (Rowell 2003). Our interest here is in understanding the mechanism by which tropical SST in particular influences Sahel rainfall.

One mechanism by which the tropical SST field can influence Sahel rainfall is by causing the intertropical convergence zone (ITCZ) to move southward. Since the Sahel lies along the northward edge of the climatological position of the ITCZ in northern summer, it receives less rainfall if the ITCZ does not migrate as far north as that climatological position. This is likely to occur if the SST in the southern tropical Atlantic increases relative to that of the northern tropical Atlantic. Biasutti and Giannini (2006) found that this scenario is typical of coupled climate model simulations run for the twentieth century, and hypothesized that the cooling of the northern hemisphere relative to that of the southern was due to the impact of anthropogenic aerosol emissions.

Here, we consider another possible mechanism, which involves the tropical mean SST rather than its gradient. This mechanism, discussed by Chiang and Sobel (2002) and Neelin et al. (2003), involves the warming of the entire tropical troposphere in response to tropical SST increases. The idea is illustrated well by the response of tropical regions remote from the central and eastern Pacific oceans to El Niño events. In those events, the central and eastern Pacific oceans warm, first driving increases in atmospheric deep convection locally. The troposphere in those regions then warms to adjust to the increased SST. Due to the large scale of geostrophic adjustment in the tropics, this warming is not localized over the regions of SST increase, but spreads so that the entire tropical troposphere warms. In remote ocean regions, where the SST has not increased, this leads to a stabilization of the atmosphere to deep convection, and a consequent reduction in precipitation (in regions which experience significant precipitation climatologically). This chain of events was illustrated by Chiang and Sobel (2002) using a single-column modeling methodology proposed by Sobel and Bretherton (2000). Neelin et al. (2003) used an intermediate-complexity climate model to simulate not only the single-column dynamics just described, but also more complex feedbacks on this involving horizontal advection of moisture and other effects.

In the coupled system, the reduction in precipitation in the remote regions leads the ocean surface to warm in order to "catch up" to the warmer free troposphere. This warming, which takes several months due to the heat capacity of the mixed layer, can be due either to decreases in surface turbulent energy fluxes (due to

either weaker winds or increased near-surface humidity, the latter being induced by convective adjustment to the warmer troposphere) or to reduced cloud cover, and thus increased surface shortwave radiation, caused by the reduction in deep convection. The roles of surface wind and solar radiation changes were discussed by Klein et al. (1999), though not connected by those authors to the tropospheric warming. Increases in downwelling surface radiation due to increased atmospheric temperature and humidity may also play a role. Once the surface catches up, the precipitation can generally be expected to return to normal, all else equal. The coupled mechanisms involved in this aspect of the response in precipitating regions are described in a number of recent studies (Chiang and Sobel 2002; Sobel et al. 2002; Su et al. 2003, 2005; Chiang and Lintner 2005; Lintner and Chiang 2006). In nonprecipitating regions, the surface response is expected to be weaker, since deep convection provides the strongest link between the boundary layer and free troposphere (Chiang and Sobel 2002). The differing responses in precipitating versus nonprecipitating regions can be expected to lead to more complex effects resulting from horizontal gradients in anomalous diabatic heating.

An essentially similar mechanism seems to operate over land during El Niño events. On average, most tropical land regions remote from the eastern Pacific dry during these events (Ropelewski and Halpert 1986; Kiladis and Diaz 1989; Mason and Goddard 2001; Lyon and Barnston 2005). This implies a mechanism which acts with the same sign over the entire global tropics, such as the tropospheric stabilization described above. The surface response over land is not quite as simple as that over the ocean, however. The precipitation response in the simulations of Chiang and Sobel (2002) was a transient response, related to the finite heat capacity of the ocean mixed layer. Over a swamp, or ocean mixed layer of infinitesimal depth, we expect essentially no remote precipitation response, at least within the assumptions of the idealized single-column view, as the surface temperature would catch up immediately to the imposed tropospheric warming. Some other source of surface "memory", besides simple heat capacity, is needed if the rainfall response to ENSO over land is to be explained in this way. One possibility is soil moisture effects, which can provide a month or two of memory, particularly in semi-arid regions such as the Sahel (Koster and Suarez 2001). Three-dimensional effects outside the single-column assumptions of Chiang and Sobel (2002) may also provide an influence over land, even in the absence of surface memory. For example, anomalous circulation

structures resulting from spatial gradients in the response between land and ocean, or different ocean regions, could result in anomalous moisture advection over land.

While the tropospheric stabilization mechanism is perhaps most easily understood in the context of ENSO, it has been argued that it can operate on longer time scales as well. Chou and Neelin (2004) argued that it can operate under global warming, and Giannini et al. (2003) and Biasutti and Giannini (2006) suggested that it may have been at least partly responsible for the Sahel drought of the 1970s and 1980s. Understanding whether this is the case has important implications for future climate change. While some coupled climate models simulate a wetter Sahel in a world warmed by anthropogenic greenhouse gas emissions, others predict a much drier one (Held et al. 2005).

Here, we use a regional climate model to address these issues. We first examine to what extent the regional model simulates the Sahel drought at all, when forced by an atmospheric general circulation model (AGCM) which in turn is forced by observed SST. Then, we perform sensitivity experiments to test the hypothesis that the SST acts on Sahel rainfall via the tropospheric temperature. The regional model framework is useful for this purpose, because it allows us to intervene in the model temperature field through the boundary conditions. Regional models have previously been used with good results over Africa (e.g., Sun et al. 1999a, b; Vizy and Cook 2002; Jenkins et al. 2005).

2 Experimental setup

We use the ECHAM4.5 AGCM (Roeckner et al. (1996), and the NCEP Regional Spectral Model v.97 (RSM97) (Juang and Kanamitsu 1994; Juang et al. 1997; Juang and Hong 2001; RSM Short Course 2005). The AGCM was configured at triangular 42 (T42) spectral truncation, giving a spatial resolution of about 2.8° latitude–longitude, with 19 vertical layers. The NCEP RSM97 with a horizontal resolution equivalent to approximately 50 km grid spacing is used to downscale the ECHAM4.5 simulations. The land surface model used in the RSM97 simulations is the NOAH (NCEP-OSU-Air Force-Office of Hydrology) Land Surface Model. The initial conditions for the land-surface are taken from the NCEP monthly mean climatology data base (Mitchell 2001; Hong 2005).

The one-way nesting of the NCEP RSM97 into the ECHAM4.5 AGCM is different from conventional methods that use global model fields only along the lateral boundary zone. The perturbation nesting method also uses the global model output over the entire regional domain, as well as in the lateral boundary zone. The dependent variables in the regional domain are defined as a sum of a base (time dependent field from the AGCM) and a perturbation (computed by the regional model). The perturbation is defined as nonzero inside the domain but zero outside the domain. Five prognostic variables from the global model outputs are used as the base fields in the RSM97. They are zonal and meridional winds, temperature, humidity, and surface pressure. All diagnostic variables (e.g., precipitation) are generated solely by the regional model (Juang et al. 1997; Camargo et al. 2006).

Multi-decadal ECHAM4.5 AGCM ensemble simulations of approximately 50 years, using observed SST, have been produced by the ECHAM4.5 AGCM (Barnston et al. 2003; Camargo et al. 2006). The regional simulations were run from July to September for the chosen wet and dry years. The ECHAM4.5 output was saved every 6 h for the nesting of the regional model.

Both models have 19 vertical levels, at the same locations, so no vertical interpolation was necessary in order to nest the RSM97 in the GCM. The regional domain has 109 grid points in zonal and 82 in meridional direction, and spans from 32.5°W to 18.9°E and 0.6°S to 35.1°N. 46 wavenumbers in the zonal direction and 35 wavenumbers in the meridional direction are retained in the RSM simulations, approximately equivalent to 50 km grid spacing, as stated above.

Three sets of RSM97 simulations have been performed, as follows.

We first performed an ensemble of seven RSM97 simulations each for the chosen wet (1955) and dry (1986) years (14 simulations total). These simulations were forced by observed SST, and by boundary and initial conditions given by different ECHAM4.5 ensemble members for the periods in question. The primary purpose of this part of the experiment was to make sure that the regional model captures the essence of the signal of interest over the Sahel; i.e., that the wet year is wet, and the dry year is dry.

Next, we performed a set of simulations designed to isolate the effects of interdecadal variability in SST on the Sahel. We used the seasonally varying decadal mean of the SSTs for the period of 1950–1959 to run seven ECHAM4.5 ensemble simulations for a period of 5 months, May–September. These were then used to force the RSM97 for July–September, producing an ensemble of seven such simulations. We refer to these as the ''1950s'' simulations. We then repeated this procedure for the period 1978–1987, producing an

ensemble of seven RSM97 simulations referred to as the "1980s" simulations. The difference between the SST used for the 1980s simulations and that used for the 1950s simulations is shown in Fig. 1. The difference reaches values as large as 0.6°C over the tropical oceans.

Finally, we performed a set of simulations designed to test the hypothesis that the influence of the tropical SST increases from the 1950s to the 1980s on the Sahel is achieved primarily via the warming of the troposphere that they induce. In these simulations, we used the initial and boundary conditions from the 1955 GCM simulation, but added a horizontally uniform, vertically varying temperature increment to the GCM temperature field before using it to force the RSM97. We used two different temperature increments: one obtained by subtracting the ensemble and tropical 20°N–20°S mean JAS temperature for 1950–1959 from that for 1978–1987, and one obtained by performing the same procedure on the NCEP/NCAR reanalysis.

3 Results

3.1 Sahel rainfall trend in the GCM simulations

Since any regional model simulation is strongly influenced by the large-scale data used to force it, we first examine the decadal rainfall variability in the EC-HAM4.5 simulations. Figure 2 shows the ensemble mean JAS precipitation from these simulations over the Sahel (here defined as 10°N–18°N and 20°W–20°E) compared to that from the CMAP data set (Xie and
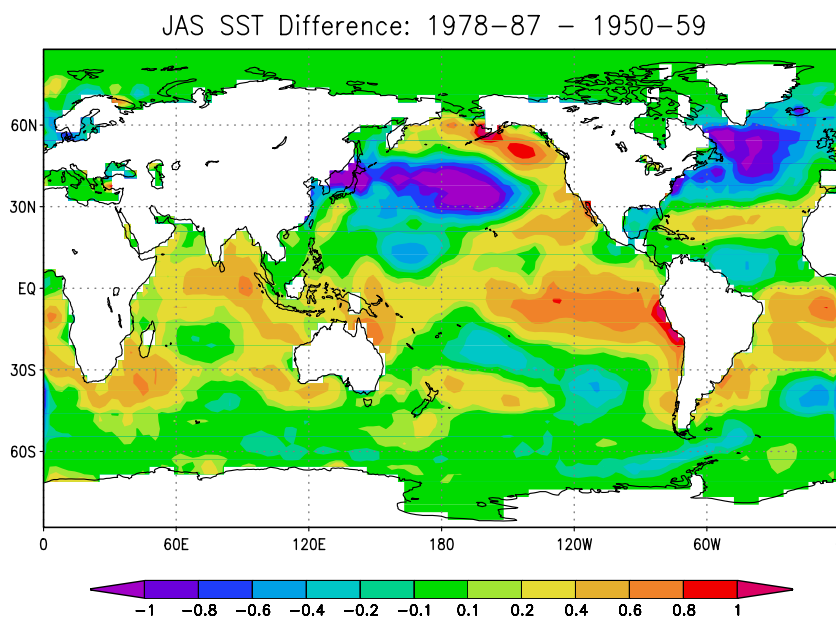
Arkin 1996). We can see that the GCM captures the sign of the observed trend, but is considerably weaker in magnitude. This figure also illustrates our reasons for choosing 1955 and 1986 as representative wet and dry years. In both years, there is good agreement between ECHAM4.5 and the observations (something not true in many individual years), and 1955 is much wetter than 1986, being anomalously wet even by comparison to the rest of the 1950s in the ECHAM4.5 simulation (though not in the observations).

3.2 RSM97 simulations of 1955 and 1986

In this section we show ensemble mean precipitation from the 1955 and 1986 simulations, and compare it to several observational data sets. The latter include the climate anomaly monitoring system (CAMS), precipitation reconstruction over land (PRECL) (Chen et al. 2002), and the CRU05 (Mitchell and Jones 2005), New et al. (1999). All of these are constructed from surface gauge observations. The nominal resolutions of the CAMS, PRECL, and CRU data sets are 2° × 2°, 2.5° × 2.5° and 0.5° × 0.5°, respectively, though in many times and places the available observations are sparse and gaps are filled in using different schemes. For this reason, and possibly others (e.g., data collection methods, instrument calibrations, different retrieval algorithms), the different data sets do not agree precisely with one another.

Figure 3 shows the spatial patterns of JAS precipitation over western Africa for the GCM, RSM97, and CRU data sets for 1955 and 1986, respectively. The ECHAM4.5 and RSM97 precipitation fields are

Fig. 1 July–September SST difference between the periods 1978–1987 and 1950–1959
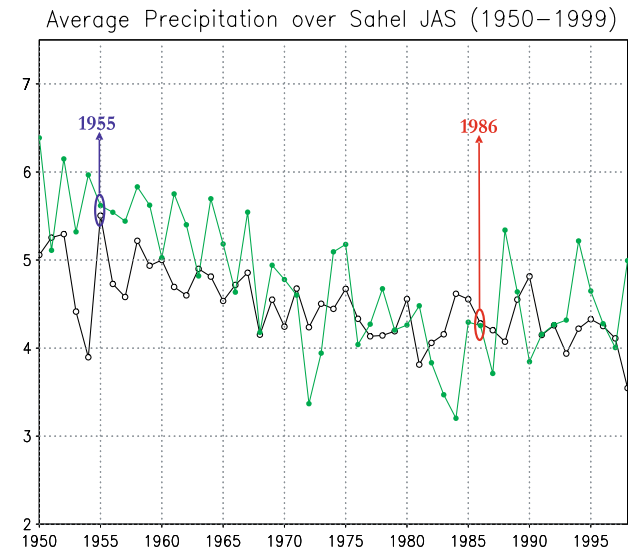
Fig. 2 ECHAM4.5 (*black*) and observed (*green*) time series for precipitation averaged over 10°N–18°N, 20° W–20°E, and the months July–September

strikingly different from one another, with the ECHAM4.5 rain being much stronger over ocean than land, and the RSM97 the reverse. The RSM97 has a more continuous band of strong precipitation across west Africa than do any of the observational data sets, which tend to show rain concentrated along the west coast between 5°–10°N, 10°–15°W, and around 5°N, 10°E. The RSM97 simulation is remarkably similar between the 2 years; the 1955 and 1986 solutions appear very similar at first glance, although there is, as the difference plot shows, a shift of the rain belt southward in 1986 compared to 1955. The 1986–1955 difference in the CRU observations is a much more nearly uniform drying over subsaharan west Africa. In both the RSM97 and the observations, the Sahel is drier in 1986 than 1955, but the spatial patterns are different. The shift in the RSM97 is evident, although weaker, in the ECHAM4.5 1986–1955 difference.

3.3 Simulations forced by decadal mean SST

Figure 4 shows the the ensemble mean of the ECHAM4.5 and RSM97 simulations forced by decadal mean SST from the 1950s and 1980s, as described above. Many of the features from the 1986 and 1955 simulations are reproduced. The ECHAM4.5 and RSM97 solutions are different, with the same reversed land–ocean contrast as before, and the two RSM97 solutions again look similar to the eye, with the difference between the 1980s and 1950s manifest as a southward shift of the rain belt in the 1980s.

In this case, however, the RSM97 result is quite similar to the CRU observations, which also show a southward shift. While we would like to believe that this is a vindication of our simulations, this is not so clear, since the CAMS and PRECL data sets do not show such a shift so clearly in the difference between these two decadal means, as shown in Fig. 5. The careful analysis of raw gauge data by Nicholson (1993) shows the trend in annual mean rainfall over this period to be negative over all of subsaharan west Africa, though stronger in the Sahel than on the Guinea coast. We might think of this as the superposition of a uniform drying and a southward shift, with the uniform drying being the stronger component. Some of the difference in the CRU data here is surely due to our restriction to the JAS season. Ward (1998, see his Fig. 6) shows that the drying trend along the Guinea coast is strongest in June and October–November, vanishing or even reversing in JAS. Our conclusion is that, while there is some disagreement among the different gridded products we have examined, the decadal precipitation changes in our RSM97 simulations bear considerable resemblance to those in the observations, with a robust drying of the Sahel, though the southward shift of the rain belt is over-emphasized compared to the uniform drying component. This provides further evidence that the Sahel drought of the 1970s and 1980s was forced by decadal changes in SST, as concluded by previous studies (Folland et al. 1986; Giannini et al. 2003; Jenkins et al. 2005; Held et al. 2005).

The design and interpretation of these experiments is based on the assumption that the response of Sahel rainfall to SST is primarily linear. Strictly, rather than performing short simulations with decadal mean SST, it would be more appropriate to perform simulations for each individual year of both decades, and then take the decadal means of the results. We have not done this. While it is possible that nonlinearities would lead to different results if we were to take the decadal mean of all the individual years in each decade rather than performing simulations with decadal mean SST, we consider the evidence in support of our primary conclusions to be fairly strong, at least within the context of this particular model. We have performed three different sorts of simulations: the individual years 1955 and 1986, those with decadal mean SST, and those with imposed tropospheric warming (below). All three lead to the same conclusion, that a warmer troposphere leads to reduced Sahel rainfall in this model. Further support of our results is given by the agreement of those results with those from with other models (e.g., Folland et al. 1986; Giannini et al. 2003; Jenkins et al.
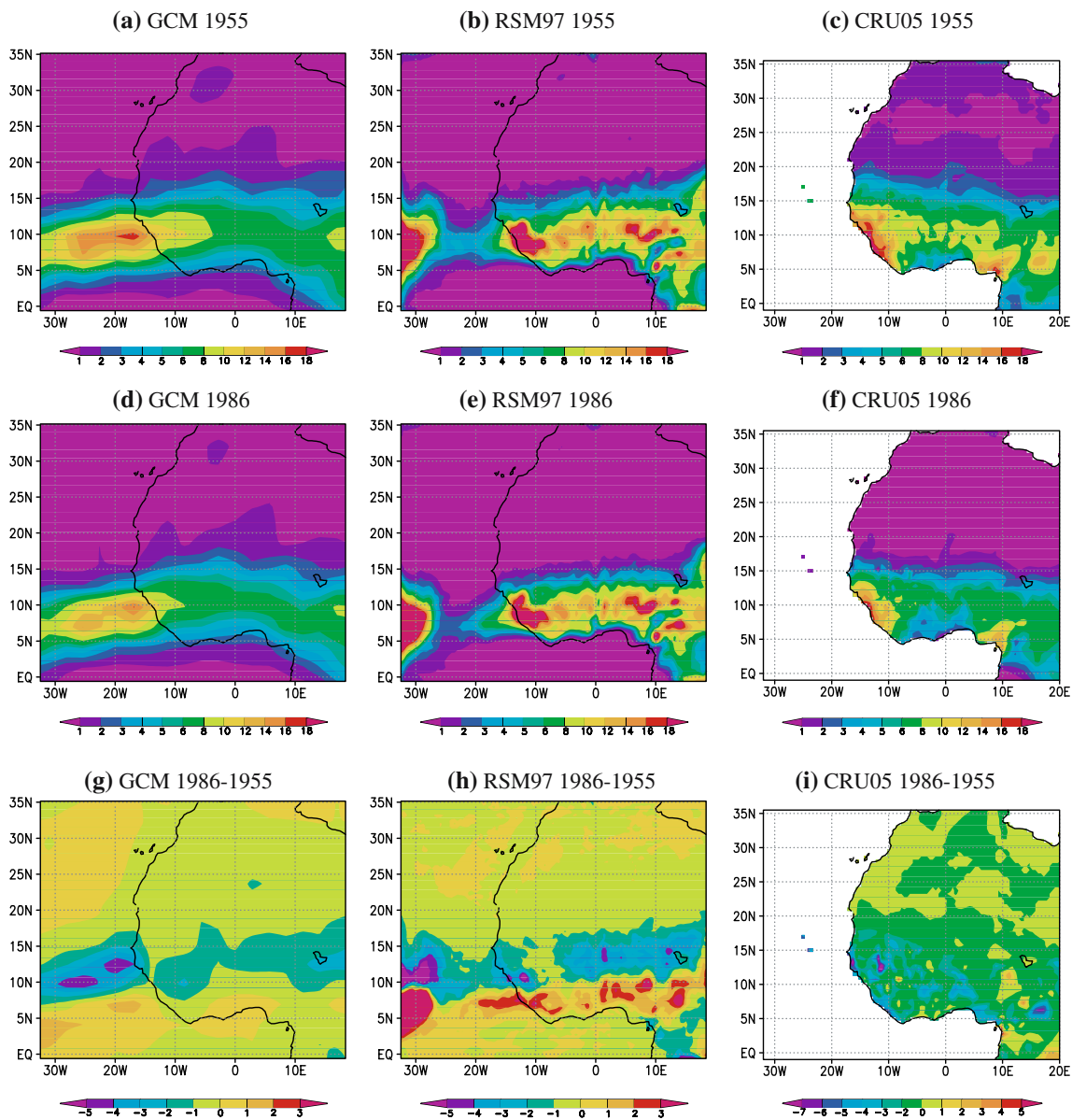
Fig. 3 July–September precipitation fields from ECHAM4.5 (*left column*), RSM97 (*center column*), and CRU05 observations (*right column*) for 1955 (*top*) and 1986 (*center*) and the difference 1986–1955 (*bottom*). For the models, the fields shown are ensemble means

2005) which show qualitatively similar responses of Sahel rainfall to the observed decadal SST changes.

3.4 Tropospheric warming simulations

In this part of the project we modified the temperature profile from the ECHAM4.5 simulations for the seven wet year regional model simulations (all ensemble members) by adding a warming profile to the ECHAM4.5 1955 temperature fields. That is, the temperature field used to force the RSM97 was

$$T(x, y, \sigma, t) = T_E(x, y, \sigma, t) + \Delta T(\sigma)$$

where $T_E(x,y,\sigma,t)$ is the ECHAM4.5 temperature field from 1955, and $\Delta T(\sigma)$ was chosen to be either (a) the difference between the tropical (20°N–20°S) mean temperature fields between the 1950s and 1980s simulated in the ECHAM4.5 model, or (b) the same difference in the NCEP reanalyses (but here only for a single ensemble member, due to small differences among ensemble members), divided by two. Figure 6 shows the ECHAM4.5 $\Delta T(\sigma)$ and NCEP $\Delta T(\sigma)$ multiplied by 0.5. We can see that the NCEP profile is very nearly moist adiabatic, while the ECHAM4.5 profile, for reasons we do not understood, is not, having a more complex vertical structure (though still an overall
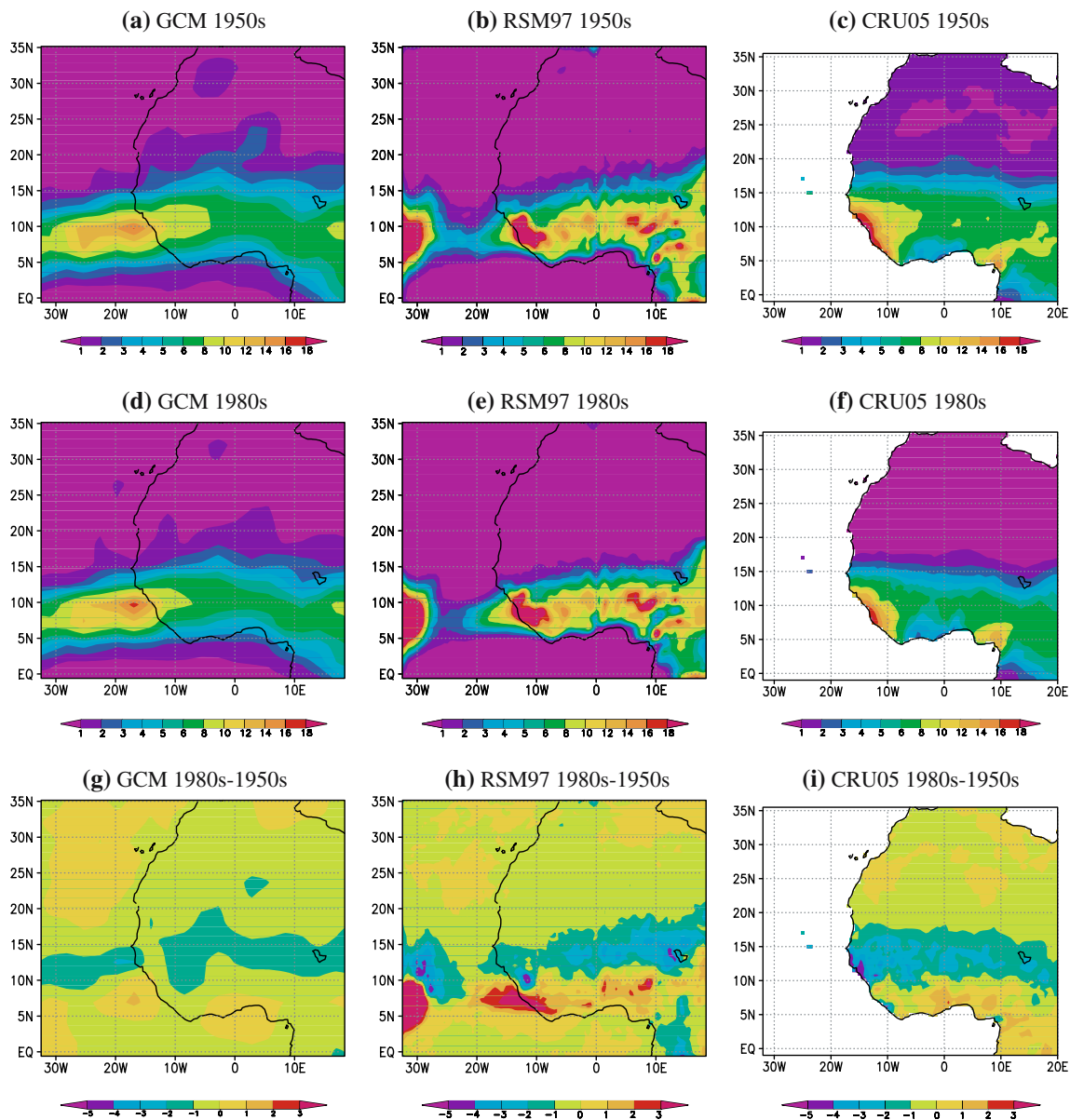
Fig. 4 As in Fig. 3, but for decadal means over the periods 1950–1959 and 1978–1987

increase with height, as would a moist adiabat). Additionally, the NCEP warming is approximately a factor of two larger than is the ECHAM4.5. To test only whether the difference in vertical structure is relevant, while removing the effect of the difference in magnitude, we divided the NCEP profile by two before adding it to the ECHAM4.5 temperature field to force the RSM97.

Figure 7 shows the precipitation field from the simulations; the one using the ECHAM4.5 ΔT is an ensemble mean, while that using the NCEP is a single simulation. Both show the drying of the Sahel, though it is more intense in the NCEP result, and the shift of the rain belt southward is more pronounced, with greater increase in rainfall along the Guinea coast. We do not understand why the modest difference in vertical structure between the two warming profiles would lead to this difference. Overall, however, these results clearly suggest that at least part of the Sahel drying in the simulations described in the previous two sections can be attributed to the warming of the troposphere in the ECHAM4.5 model.

The response of the regional model ensemble simulations is robust for all of the above described experiments; they all show a drying trend over the Sahel. The regional model ensemble correlation
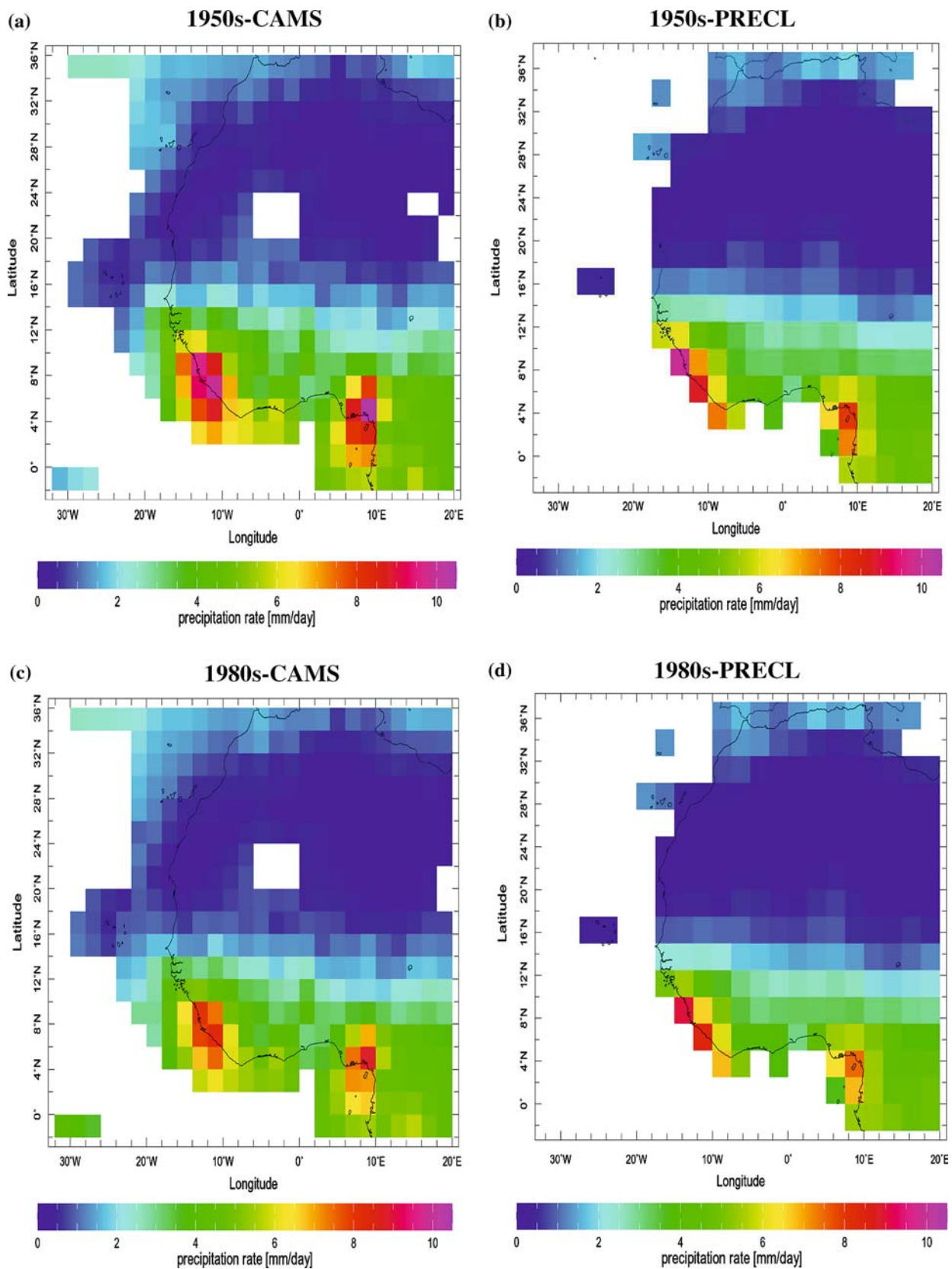
Fig. 5 Decadal mean July–September precipitation fields from the CAMS (*left*) and PRECL (*right*) data sets, for the 1950s (*top*), 1980s (*center*), and the difference 1980s–1950s (*bottom*)
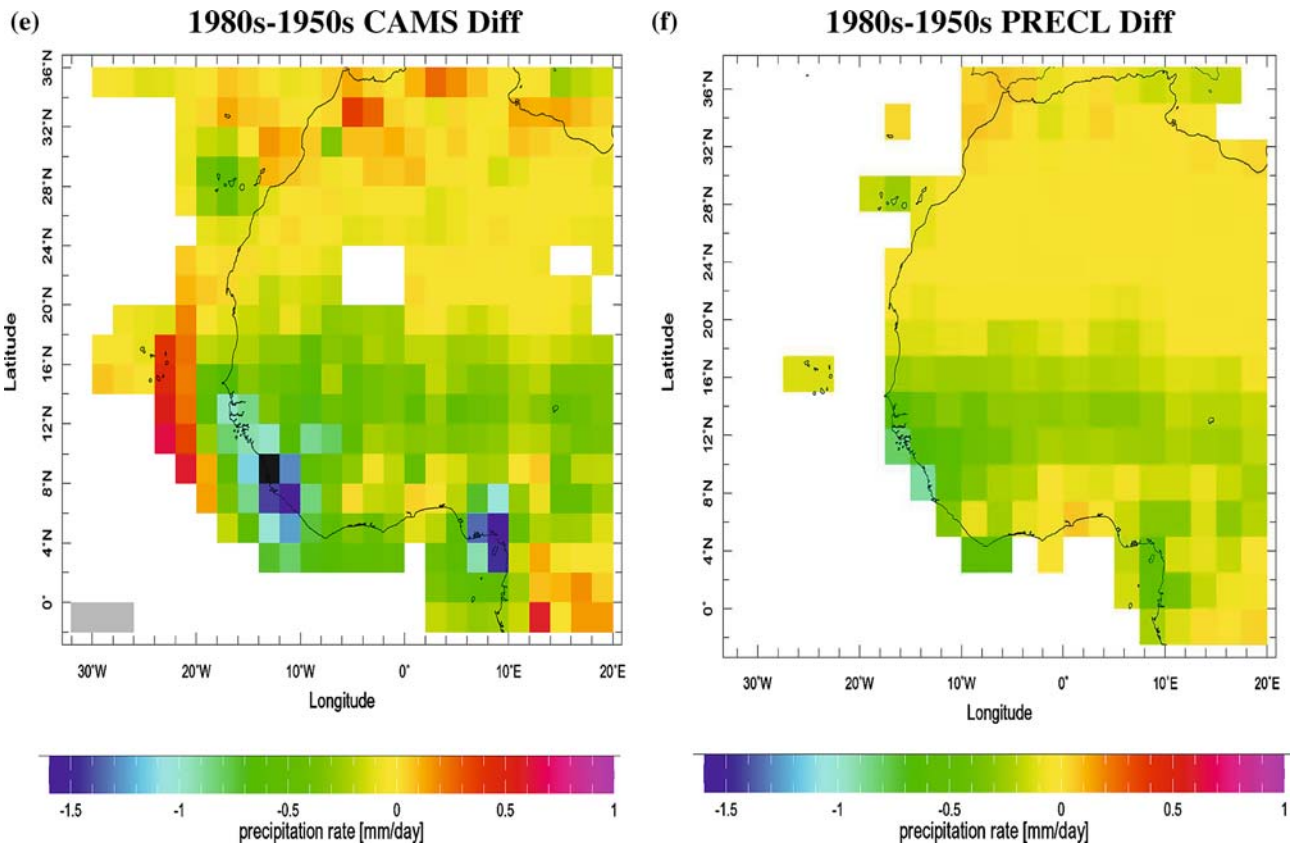
Fig. 5 continued

ranges from 92 to 96% showing a high spatial agreement between ensembles of each of the parts of the experiments.
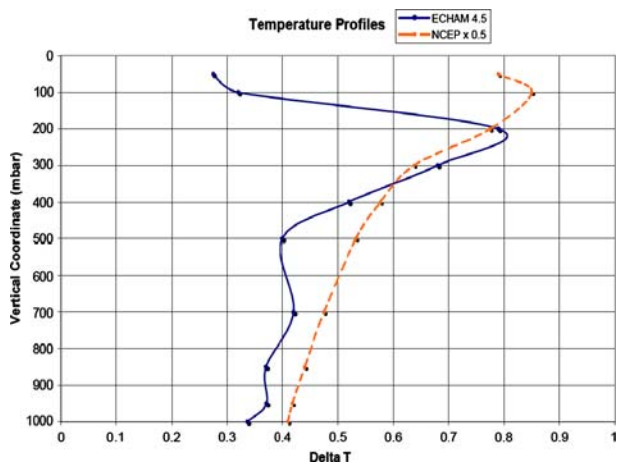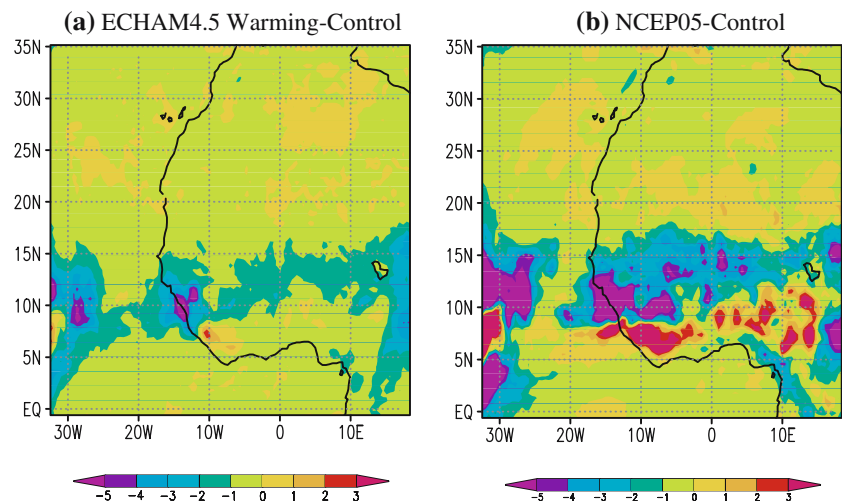

Fig. 6 Tropical mean temperature profile for the 1980s minus that for the 1950s, from the ECHAM4.5 simulations; and the same profile from the NCEP/NCAR reanalyses (courtesy of Dr. Michela Biasutti), but adjusted to similar magnitude as ECHAM4.5 profile (showing NCEP × 0.5)

4 Conclusions

We have performed a set of regional model simulations with the goal of moving towards a mechanistic understanding of the causes of the drought in the Sahel during the 1970s and 1980s. Our simulations used the NCEP regional spectral model (RSM97) forced by simulations with the ECHAM4.5 GCM, itself forced by observed SST. We performed simulations for JAS 1955 and 1986, idealized simulations forced by decadal mean SSTs from 1950–1959 to 1978–1987, and sensitivity experiments with the RSM97 forced by 1955 ECHAM4.5 boundary and initial conditions but with a horizontally uniform increase added to the temperature field. The main conclusions are as follows.

- Although the RSM97 simulations show some differences from observations, they reproduce the Sahel drought of the 1970s and 1980s very robustly. This suggests that the drought was forced by decadal changes in sea surface temperature, as found by previous studies.
- The sensitivity experiments suggest that the SST changes act on the Sahel at least in part through the warming of the troposphere which they induce.

Fig. 7 a July–September precipitation field for 1955 with the horizontally uniform warming applied, minus that from the control 1955 simulation; b the same, but for NCEP/NCAR warming profile multiplied by 0.5. The vertical profiles used for these warming simulations are shown on Fig. 6

Our interpretation of the results shown above is that at least in our simulations, the Sahel drought of the 1970s–1980s was induced by decadal increases in tropical SST. These SST increases led to an increase in the tropospheric temperature. This tropospheric temperature increase in turn was at least in part responsible for the changes in precipitation over the Sahel. Clearly, however, the mechanisms involved must be at least somewhat more complex than those described by Chiang and Sobel (2002). While the tropospheric temperature increase can be expected to stabilize the atmosphere over the Sahel to deep convection, the same can be said over the rest of the region as well, so this alone should lead to a uniform decrease in precipitation, including over the Guinea coast. The shift we see in the RSM97 (and perhaps, to some extent, in the observations for JAS) clearly cannot be explained purely in terms of the tropospheric stabilization by itself. Since the tropospheric temperature is the control parameter in our simulations, it still is likely that the tropospheric stabilization is the ultimate cause of the precipitation changes, but the proximate causes may involve more subtle feedbacks, such as described by Neelin et al. (2003) and Chou and Neelin (2004). Indeed, these studies predict drying particularly along the margins of convective zones, such as the Sahel, due to enhanced dry advection, an indirect result of the stabilization. More detailed analysis, such as construction of a moist static energy budget as done in those studies, would be necessary in order to verify whether this feedback is active.

The response of the land surface is another subtle issue. The initial land surface conditions are the same in all our simulations. This means that in our simulations for the 1980s, the land surface has not been influenced by

the atmospheric history during the intervening years. It has not been able to adjust to the changes in temperature, precipitation, and other variables. At the same time, it is not obvious to us what that response would be, and thus how this limitation of our simulations may affect the results. Since the "memory" of the land surface lies mainly in soil moisture, rather than temperature (Koster and Suarez 2001), it is far from clear that the land surface would "catch up" to the warmer troposphere, in the sense of driving the moist static energy or equivalent potential temperature of near-surface air higher to maintain the level of convective instability, in the way that an ocean mixed layer does (Chiang and Sobel 2002; Sobel et al. 2002; Su et al. 2003, 2005; Chiang and Lintner 2005; Lintner and Chiang 2006). Perhaps the drier land surface resulting from an initial warming-induced precipitation decrease would instead provide a positive feedback, leading to still greater reduction in precipitation.

References

Barnston AG, Mason SJ, Goddard L, DeWitt DG, Zebiak SE (2003) Multimodel ensembling in seasonal climate forecast-

ing at IRI. Bull Am Meteorl Soc 84(12):1783–1796 http://dx.doi.org/10.1175/BAMS-84-12-1783

Biasutti M, Giannini A (2006) Robust Sahel drying in response to late 20th century forcings. Geophys Res Lett (in press)

Camargo SJ, Li H, Sun L (2006) Feasibility study for downscaling seasonal tropical cyclone activity using NCEP Regional Spectral Model. Intl J Clim (in press)

Charney JG (1975) Dynamics of deserts and draught in Sahel. Q J R Met Soc 101:193–202

Chen M, Xie P, Janowiack J, Arkin PA (2002) Global land precipitation: a 50-yr monthly analysis based on gauge observations. J Hydrometeorl 3:249–266

Chiang JCH, Lintner BR (2005) Mechanisms of remote tropical surface warming during El Niño. J Clim 18:4130–4149

Chiang JCH, Sobel AH (2002) Tropical tropospheric temperature variations caused by ENSO and their influence on the remote tropical climate. J Clim 15:2616–2631

Chou C, Neelin JD (2004) Mechanisms of global warming impacts on regional tropical precipitation. J Clim 17:2688–2701

Folland CK, Palmer TN, Parker DE (1986) Sahel rainfall and worldwide sea temperatures 1901–85. Nature 320:602–607

Giannini A, Saravanan R, Chang P (2003) Oceanic forcing of Sahel rainfall on interannual to interdecadal time scales. Science 302:1027–1030

Held IM, Delworth TL, Lu J, Findell KL, Knutson TR (2005) Simulation of Sahel drought in the 20th and 21st centuries. Proc Natl Acad Sci USA 0: 0509057102

Hong SY (2005) Physical processes in atmospheric model-NCEP MRF/RSM physics. (available from http://www.ecpc.ucsd.edu/projects/RSM)

Jenkins GS, Gaye AT, Sylla B (2005) Late 20th century attribution of drying trends in the Sahel from the regional climate model (RegCM3). Gephys Res Lett 32: http://dx.doi.org/10.1029/2005GL024225

Juang H, Hong SY (2001) Sensitivity of the NCEP regional spectral model to domain size and nesting strategy. Mon Weather Rev 129:2904–2922

Juang H, Kanamitsu M (1994) The NMC nested regional spectral model. Mon Weather Rev 122:3–24

Juang H, Hong SY, Kanamitsu M (1997) The NCEP regional spectral model: an update. Bull Am Meteorl Soc 78:2125–2143

Kiladis GN, Diaz HF (1989) Global climate anomalies associated with extremes in the southern oscillation. J Clim 2:1069–1090

Klein SA, Soden BJ, Lau NC (1999) Remote sea surface temperature variations during ENSO: evidence for a tropical atmospheric bridge. J Clim 12:917-932

Koster RD, Suarez MJ (2001) Soil moisture memory in climate models. J Hydrometeorol 1:558–570

Lintner BT, Chiang JCH (2006) Adjustment of the remote tropical climate to El Niño conditions. J Clim (in press)

Lough JM (1986) Tropical Atlantic sea surface temperatures and rainfall variations in subsaharan Africa. Mon Weather Rev 14:561–570

Lyon B, Barnston AG (2005) ENSO and the spatial extent of interannual precipitation extremes in tropical land areas. J Clim 18:5095–5109

Mason SJ, Goddard L (2001) Probabilistic precipitation anomalies associated with ENSO. Bull Am Meteorl Soc 82:619–638

Mitchell K (2001) The community NOAH land–surface model (LSM). (available from http://www.emc.ncep.noaa.gov/mmb/gcp/noahlsm)

Mitchell T, Jones P (2005) An improved method of constructing a database of monthly climate observations and associated high-resolution grids. Int J Climatol 25:693–712

Neelin JD, Chou C, Su H (2003) Tropical drought regions in global warming and El Niño teleconnections. Geophys Res Lett 30(24): http://dx.doi.org/10.1029/2003GLO018625

New M, Hulme M, Jones P (1999) Representing twentieth-century space-time climate variability. Part I: development of a 1961–90 mean monthly terrestrial climatology. J Clim 12:829–856

Nicholson S (1993) An overview of African rainfall fluctuations of the last decade. J Clim 6:473–487

Palmer TN (1986) Influence of the Atlantic, Pacific and Indian oceans on Sahel rainfall. Nature 322:251–253

Roeckner E, Arpe K, Bengtsson L, Christoph M, Claussen M, Duemenil L, Esch M, Giorgetta M, Schlese U, Schulzweida U (1996) The atmospheric general circulation model ECHAM-4: model description and simulation of present-day climate. Tech. Rep. 218, Max-Planck Institute for Meteorology, Hamburg, p 90

Ropelewski CF, Halpert MS (1986) Global and regional scale precipitation patterns associated with the El Niño/Southern Oscillation. Mon Weather Rev 115:1606–1626

Rowell DP (2003) The impact of Mediterranean SSTs on the Sahelian rainfall season. J Clim 16:849–862

RSM short course: GSM/RSM basics (2005) (available online from http://www.ecpc.ucsd.edu/projects/RSM)

Sobel AH, Bretherton CS (2000) Modeling tropical precipitation in a single column. J Clim 13:4378–4392

Sobel AH, Held IM, Bretherton CS (2002) The ENSO signal in tropical tropospheric temperature. J Clim 15:2702–2706

Su H, Neelin JD, Meyerson JE (2003) Sensitivity of tropical tropospheric temperature to sea surface temperature forcing. J Clim 16:1283–1301

Su H, Neelin JD, Meyerson JE (2005) Tropical tropospheric temperature and precipitation response to sea surface temperature forcing. In: Wang JCC, Xie S-P, (ed) Ocean–atmosphere interaction and climate variability, vol 147 of geophysical monograph series, American Geophysical Union, pp 379–392

Sun L, Semazzi FHM, Giorgi F, Ogallo L (1999a) Application of the NCAR regional climate model to eastern Africa, 1, Simulation of the short rains of 1988. J Geophys Res 104:6529–6548

Sun L, Semazzi FHM, Giorgi F, and Ogallo L (1999b) Application of the NCAR regional climate model to eastern Africa, 2, Simulation of interannual variability of short rains. J Geophys Res 104:6549–6562

Thiaw WM, Bell GD (2005) Mechanisms associated with the June–September 2003 Sahel rainfall and implications for seasonal climate forecasts. CLIVAR Exch 10(1):2931

Vizy EK, Cook KH (2002) Development and application of a mesoscale climate model for the tropics: influence of sea surface temperature anomalies on the West African monsoon. J Geophys Res 107, http://dx.doi.org/10.1029/2001JD000686

Ward MN (1998) Diagnosis and short lead time prediction of summer rainfall in tropical north Africa at interannual and multidecadal timescales. J Clim 11:3167–3190

Xie P, Arkin PA (1996) Analysis of global monthly precipitation using gauge observation satellite estimates, and numerical predictions. J Clim 9:840–858